

Development and Verification of a Narrowband High-Power Microwave Test Asset

D. Elkins* and J. Fortinberry

Redstone Technical Test Center, Redstone Arsenal, Alabama 35898

Many commercial and military systems are complex networks of electronic monitoring and control subsystems, including vehicles, aircraft, and even the modern power grid. Coupled with the explosion of wireless devices and the potential for front- and backdoor radio frequency (RF) coupling into these modern systems, susceptibility to high-intensity RF environments generated by high-power microwave (HPM) sources and weapons is becoming a focused concern for Department of Defense Electromagnetic Environmental Effects testers and evaluators. To better characterize the HPM threat and its effects on modern Army electronic systems and to begin development of appropriate HPM test assets to emulate this threat, Redstone Technical Test Center has retrofitted its RADAR Environment Emulation System to generate high-intensity fields that would be common to narrowband and mesoband HPM sources. This HPM test source has been utilized to evaluate the effects of RF on various types of electronic components to include computers, cell phones, and handheld radios. Results that detail variations in the test parameters and their related effects on the electronic subsystems to determine upset and failure levels are presented.

KEYWORDS: Directed energy, High-power microwave, Narrowband, Test and evaluation

1. Introduction

Much previous research has been focused on developing multigigawatt high-power microwave (HPM) sources capable of producing pulse widths (PWs) of less than 100 ns and fields on the order of 10 kV/m at distances greater than 1 km (Refs. 1 and 5). These weapons could be used against hostile forces to disrupt military infrastructure, such as communication, command, and control networks, without causing civilian casualties. However, an even greater threat, especially to the commercial sector, could be the suitcase-sized mesoband HPM systems that are currently available for purchase. For example, the DS110 system manufactured by DIEHL Corporation in Germany will emit a peak electric field of 125 kV/m measured at a distance of 1 m (Ref. 3). These systems are small enough to be carried into buildings and could cause disruption or damage to key commercial interests such as computer networks. Previous work has shown that modern personal computers (PCs) can suffer upsets at levels as low 0.5 kV/m (Refs. 4 and 6). However, previous studies did not fully examine the effects of the PW or the pulse repetition frequency (PRF) on the systems.

Received April 1, 2008; revision received August 20, 2008.

*Corresponding author; e-mail: David.Elkins@us.army.mil.

Table 1. REES magnetron characteristics

Frequency (MHz)	Peak power (kW)	PW (μ s)	Maximum duty cycle
750–1,000 (UHF oscillator)	200	0.5–4	0.001
1,220–1,350	650	0.5–4	0.001
1,250–1,310	1,600	0.5–4	0.001
2,900–3,100	840	0.5–4	0.001
2,900–3,100	2,600	0.5–4	0.001
5,400–5,800	230	0.5–4	0.001
5,400–5,800	1,000	0.5–4	0.001
8,500–9,600	350	0.5–4	0.001
14,800–15,200	200	0.1–0.35	0.001
24,250	35	0.1	0.0003
35,050	200	0.1	0.0003

2. Setup

Redstone Technical Test Center (RTTC) has developed multiple high-power, pulsed-amplifier systems for the purpose of evaluating the effects of extremely high-level electric-field environments on military weapon systems. The potential susceptibility of modern digital electronics to damage and upset from peak electric fields has required the test community to develop assets that will emulate battlefield radio frequency (RF) systems. Of particular concern are flight-critical components for aviation and ground-based command and control centers that are necessary for mission readiness and network-centric warfare.

Because of the ability of RTTC to develop high-power pulsed RF environments, three of the RADAR Environment Emulation System (REES) bands were chosen for this investigation and are shown in boldface in Table 1. Also, the bands allow some freedom in varying key parameters such as PW and PRF. Of particular interest was the lowest band of 1.25–1.31 GHz, which represented frequencies that are nearest the frequency spectrum of modern computer clocks and cell phones.

The REES is a magnetron-based amplifier system developed to emulate the electromagnetic environments characteristic of RADAR systems and utilized as a test and evaluation tool to analyze the effects of pulsed RF environments on the functionality and survivability of weapon electronics. The REES houses 10 magnetrons and an ultra-high-frequency oscillator that cover discrete portions of the frequency band from 750 MHz to 35 GHz. The frequency and PW are continuously variable throughout each band (as defined in Table 1). Table 1 lists the general RF characteristics of the REES operating bands to include peak output power, PW, frequency bandwidth, and maximum duty cycle.

To achieve RF output, the REES uses a pulsed generator as the user interface to set up and define the pulse characteristics for a given output. A pulsed transformer is utilized to provide the appropriate amplitude input required to drive a hard-tube modulator, which in turn drives the output magnetron at the specified voltage and pulsed duty cycle. The hard-tube modulator utilizes a tetrode vacuum tube to discharge a 1- μ F capacitor through the magnetron in order to produce a high-power RF pulse. The system high-voltage supply is integrated as part of the hard-tube modulator and supplies power to all of the magnetrons as well as the modulator. System control and automation are accomplished by a programmable logic controller (PLC) that serves as the automated control of the RF output, timing, safety

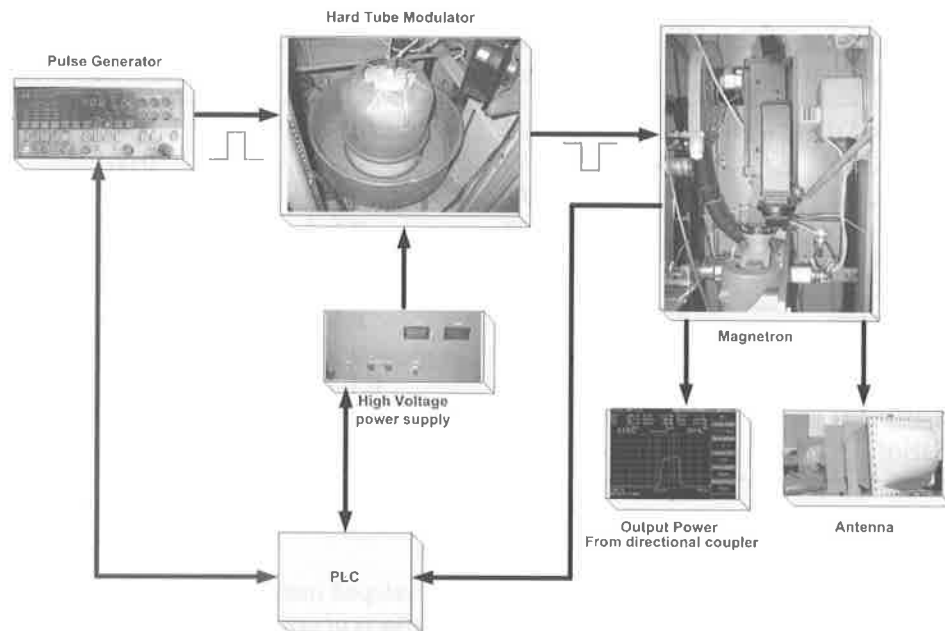


Fig. 1. REES block diagram.

interlock, and RF monitoring subsystems. Figure 1 is a conceptual block diagram illustrating the operational flow of the REES.

In general, the REES PWs can be varied from 500 ns to 4 μ s. To avoid damage to the magnetrons, the maximum duty cycle is controlled by the PLC and never allowed to exceed 0.001. Of course, these values vary for each individual magnetron as demonstrated in Table 1. A distilled-water cooling subsystem is integrated with the REES and provides the appropriate cooling required for higher-power magnetrons. To avoid breakdown in the waveguide and antennas, these systems are sealed and pressurized. Finally, the recommended RF parameter curve for the 1.3-GHz magnetron used in this investigation is shown in Figure 2 and details the required input current and voltage necessary at the anode to realize a given peak output power.

Figure 2 illustrates the recommended anode current/voltage parameters for the 1.3-GHz magnetron with a potential peak output power of 2.6 MW, which is the region of operation used during these measurements. It should be noted that the quality of the RF output pulse begins to deteriorate at a fairly rapid rate as the high-voltage input to the magnetron is reduced below the optimum level designed by the manufacturer. High-power variable attenuators on the RF output are required in order to obtain a dynamic range in RF output power of greater than 3 dB without compromising the output integrity of the pulse shape. Dynamic variability in output power is not a large issue for directed energy weapons intended to inflict damage or upset where maximum power is necessary; however, it is critical for evaluating the threshold levels at which electronic components, subsystems, and systems will survive and operate in the test and evaluation community.

As stated earlier, three specific bands, as highlighted in Table 1, from the REES were utilized to develop the environments required for this investigation. A set of standard-gain horns was used for the transmit antenna and a 1–18-GHz double-ridged horn was used as

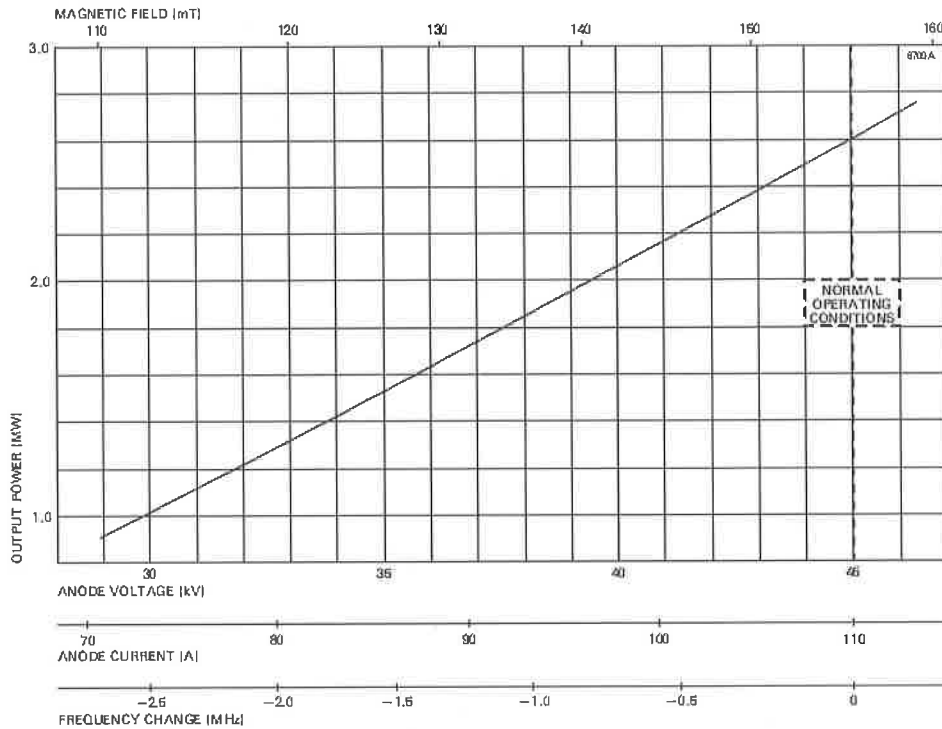


Fig. 2. 1.3-GHz magnetron input/output parameters.

the receive antenna for the purpose of measuring the received power at the test location. Power measurements were performed using a peak-power analyzer and measured without the test item present in order to establish a free field calibration. The measured power was converted to an equivalent E-field using Eqs. (1) and (2):

$$P_d \text{ (W/m}^2\text{)} = \left(\frac{4\pi}{\lambda^2 G} \right) P_r, \tag{1}$$

$$\text{E-field (V/m)} = \sqrt{120\pi P_d}, \tag{2}$$

where P_r (W) = power received plus cable losses and attenuation, λ (m) = wavelength of transmit frequency, G = gain of receive antenna, and P_d (W/m²) = power density.

Future upgrades to REES will include high-power variable attenuators on the output to allow an extended dynamic power output range beyond the current capability and to enhance the ability to threshold anomalies and a pulse-shaping network to truncate the falling edge of the output pulses.

The captured RF output pulses from each of the magnetrons used are shown in Figs. 3–5. The pulses shown represent the received output power measured at the location of the test item without accounting for cable loss, coupler attenuation, and external attenuation at the input to the peak power analyzer.



Fig. 3. 1.3-GHz RF pulse.



Fig. 4. 3-GHz RF pulse.



Fig. 5. 5.8-GHz RF pulse.

Table 2. HPM test parameters

Frequency (GHz)	PW (μ s)	PRF (Hz)
1.3	0.8–4	10
3.0	0.8–4	10
5.8	0.8–2	10

Table 3. HPM test assets

Test asset	Description
Computer 1	450 MHz, Pentium II
Computer 2	1.0 GHz, Pentium III
Computer 3	1.6 GHz, Pentium IV
Cell phone 1	Modern cell phone
Cell phone 2	Modern cell phone
Cell phone 3	Modern cell phone
Monitor 1	Cathode ray tube monitor
Monitor 2	Cathode ray tube monitor
Handheld radio 1	FRS radio
Handheld radio 2	FRS radio

3. Results

Three test frequencies were chosen to test common consumer electronic devices. These frequencies were chosen within the bands at which the REES produced the highest output power and were 1.3, 3.0, and 5.8 GHz. There was no attempt to choose frequencies that matched operating or resonant frequencies of the devices that were being irradiated. For each frequency, the electric field, PW, and antenna polarization were varied to determine differences in upset and failure levels. The test parameters of each frequency are detailed in Table 2.

The test assets that were used included an array of common consumer electronic devices. These devices were turned on and placed in the previously calibrated test locations. The electronic devices were monitored remotely with a high-resolution camera placed behind the radiating horn, and all upsets and failures were noted. The test assets are detailed in Table 3, and Figs. 6 and 7 show various test setups.

For each test item, the E-field, PW, and antenna polarization were varied and the effects were noted. Even though the PWs were varied as shown in Table 2, only the maximum PWs are listed in Tables 4–6 because the worst-case effects always occurred at the maximum PW. It is also worth noting that initially, the PRF was changed, but after numerous test runs with seemingly no effect, it was kept at a constant 10 Hz. Owing to the limited number of assets, not all of the test items were tested at each frequency. Results from the testing are shown in Tables 4–6.

Tables 4–6 show the effects of the radiated field on each of the devices tested. The results from each test point were classified into one of three categories: no observable effect (NOE),

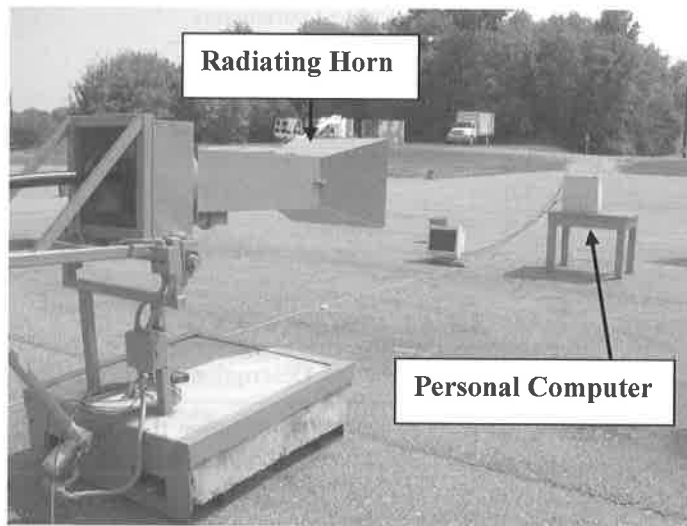


Fig. 6. 1.3-GHz computer test setup.

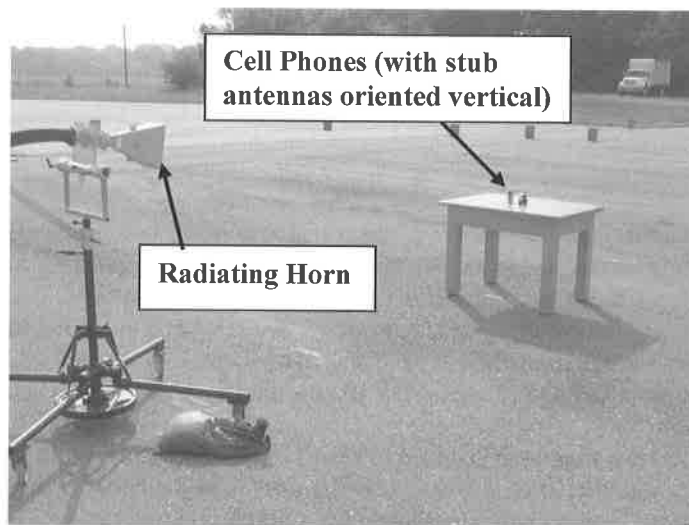


Fig. 7. 5.8-GHz cell phone test setup.

upset, or failure. NOE defines a condition in which the device being radiated exhibited no upsets during or after exposure to the HPM source. An upset is defined as a condition in which the electronic device was rendered inoperable (i.e., locked up, rebooted, or turned off) due to the HPM source but was functional after the HPM source was removed and a manual or automatic power-off/power-on sequence was performed. A failure is defined as a condition in which the electronic device was rendered inoperable by the HPM source and could not recover once the HPM source was removed.

Table 4. 1.3-GHz test results

Frequency (GHz)	Polarization	Peak E-field (kV/m)	Avg E-field (V/m)	PW (μ s)	Computer 2	Monitor 2	Cell Phone 3
1.3	V	48.9	309	4	Upset	Failure	
1.3	H	48.9	309	4	Upset	Upset	
1.3	V	16.3	103	4	Upset	Upset	
1.3	H	16.3	103	4	Upset	Upset	
1.3	V	10.9	69	4	Upset	Upset	Failure
1.3	H	10.9	69	4	Upset	Upset	
1.3	V	5.8	37	4	Upset	Upset	
1.3	H	6.2	39	4	Upset	Upset	
1.3	V	4.9	31	4	Upset	Upset	
1.3	H	5.3	34	4	Upset	Upset	
1.3	V	3.2	20	4	Upset	Upset	
1.3	V	0.5	3	4	Upset	Upset	

Table 5. 3.0-GHz test results

Frequency (GHz)	Polarization	Peak E-field (kV/m)	Avg E-field (V/m)	PW (μ s)	Computer 1	Computer 2	Computer 3	Cell Phone 1	Cell Phone 2	FRS 1	FRS 2
3	V	51.9	328	4	Upset	Upset	Failure	NOE	NOE	Failure	Failure
3	H	53.1	336	4	Upset	Upset	No Data	Upset	Upset	Upset	Upset
3	V	17.3	109	4	Upset	Upset	Upset	NOE	NOE	Upset	Upset
3	H	17.7	112	4	Upset	Upset	Upset	NOE	NOE	Upset	Upset
3	V	10.8	68	4	NOE	Upset	Upset	NOE	NOE	NOE	NOE
3	H	11.3	71	4	NOE	Upset	Upset	NOE	NOE	NOE	NOE
3	V	7.0	44	4	NOE	NOE	NOE	NOE	NOE	NOE	NOE
3	H	6.6	42	4	NOE	NOE	NOE	NOE	NOE	NOE	NOE
3	V	5.3	34	4	NOE	NOE	NOE	NOE	NOE	NOE	NOE
3	H	6.7	42	4	NOE	NOE	NOE	NOE	NOE	NOE	NOE

Table 6. 5.8-GHz test results

Frequency (GHz)	Polarization	Peak E-field (kV/m)	Avg E-field (V/m)	PW (μ s)	Computer 1	Computer 2	Monitor 1	Cell phone 1	Cell phone 2
5.8	V	47.7	213	2	Upset	Upset		NOE	NOE
5.8	H	51.0	228	2	Upset	Upset	Failure	Upset	NOE
5.8	V	15.9	71	2	NOE	Upset	Upset	NOE	NOE
5.8	H	17.0	76	2	NOE	Upset	Upset	NOE	NOE
5.8	V	10.8	48	2	NOE	NOE	Upset	NOE	NOE
5.8	H	11.0	49	2	NOE	NOE	Upset	NOE	NOE
5.8	V	7.2	32	2	NOE	NOE	Upset	NOE	NOE
5.8	H	6.5	29	2	NOE	NOE	Upset	NOE	NOE
5.8	V	4.7	21	2	NOE	NOE	Upset	NOE	NOE
5.8	H	2.9	13	2	NOE	NOE	Upset	NOE	NOE

4. Conclusions

Although the data collected during this research were from an extremely small sample of products, they show general trends. As the frequency decreased, the upset threshold level also decreased. This could be due to the lower frequencies being closer to the operating frequency of the device; it should be noted that no attempt was made to match the target operating or resonant frequencies to the HPM source frequency. The upset level at lower frequencies was evident in both the cell phone and the computer. Also, as the PW increased, upsets were observed at lower peak electric fields. Although it can be argued that by increasing the PW, and in turn the duty cycle, the average electric field is increasing and is therefore causing the upset; this scenario is unlikely due to the lack of issues when the PRF was changed. By increasing the PRF, and in turn the duty cycle, there was seemingly no effect on the upset level. The more likely cause of the lower susceptibility level lies in the characteristics of the first pulse of the pulse train. By increasing the PW, the energy level of each individual pulse also increases. It must be noted that the duty cycle for this research was on the order of 10^{-5} ; however, if the duty cycle were several orders of magnitude greater, the PRF most likely would play a greater role in damaging equipment due to thermal stacking.² Finally, the electric field polarization had no noticeable effect on the upset level of the test items except in the case of the cell phone in which horizontal polarization caused a number of upsets that were not evident with vertical polarization.

As previous research has suggested, it is quite difficult to permanently damage PCs.⁴ In addition, this research showed that even common electronic devices such as cell phones and handheld radios were quite robust to HPM, at least at the higher frequencies. The damage to one computer occurred at a level of 50 kV/m, and it occurred to the hard drive of the computer. However, computer upsets occurred frequently at much lower electric field levels and did not seem to be polarization specific. The computer upsets included automatically rebooting, shutting down, and locking up, and in the 1.3-GHz case, the computer was susceptible at peak electric fields as low as 0.5 kV/m. Computer monitors showed more susceptibility than the computers. Upsets included screen blinking as well as blacking out, and the text on the monitor screens was unreadable at all test points. The cell phone as well as the Family Radio Services (FRS) radio failures included damage to the display and internal component damage.

References

- ¹Agee, F.J., IEEE Trans. Plasma Sci. **26**(June), 235 (1998).
- ²Backstrom, M.G., and K.G. Lovstrand, IEEE Trans. Electromagnetic Compatibility **46**(August), 396 (2004).
- ³Baum, C.E., D. Nitsch, W.D. Prather, F. Sabath, and R.J. Torres, IEEE Trans. Electromagnetic Compatibility **46**(August), 335 (2004).
- ⁴Carter, N.J., D. Herke, R. Hoad, and S.P. Watkins, IEEE Trans. Electromagnetic Compatibility **46**(August), 390 (2004).
- ⁵Giri, D.V., and F.M. Tesche, IEEE Trans. Electromagnetic Compatibility **46**(August), 322 (2004).
- ⁶Radasky, W.A., "The Threat of Intentional Electromagnetic Interference (IEMI) to Wired and Wireless Systems," 17th International Zurich Symposium on Electromagnetic Compatibility, March 2006.

The Authors

Mr. David Elkins attended Auburn University from 1984 to 1989 and graduated with a Bachelor of Electrical Engineering Degree in 1989. He has been employed by Redstone Technical Test Center, an independent Army research/test lab, since graduation. In 1996, he

transitioned into a senior research engineering position and continues in that role. His major areas of focus include high-power amplifier systems and system-level electromagnetic effects. Mr. Elkins also graduated from the Auburn University Executive MBA program in 2001 with a focus on technology development/management.

Mr. Jarrod Fortinberry attended Mississippi State University from 2000 to 2005 and graduated with a Bachelor of Science degree in electrical engineering in 2005. He is currently enrolled at Mississippi State University and is pursuing a Master of Science in electrical engineering at the James Worth Bagley College of Engineering. He is employed by the Redstone Technical Test Center in Huntsville, Alabama, where he has been working as a test engineer since 2005. His specific fields of interest include high-power pulsed systems and antenna design and measurements.